Acoustic Emission Monitoring of Debonding of External Reinforcing Patches from Concrete

Dimitrios AGGELIS[1], Eleni TSANGOURI[1], Svetlana VERBRUGGEN[1],
Tine TYSMANS[1], Danny VAN HEMELRIJCK[1]
[1]Department of Mechanics of Materials and Constructions, Vrije Universiteit Brussel,
Pleinlaan 2, 1050 Brussels, Belgium

Abstract. The present study concerns the characterization of the fracture process in concrete beams which are externally reinforced by means of composite materials. The reinforcement comes in the form of CFRP (Carbon Fiber Reinforced Polymer) strip and TRC (Textile Reinforced Cement) layer. In order to monitor the accumulation of fracture beneath the non-transparent layer, AE (Acoustic Emission) sensors are used. The results show that the different mechanisms starting from concrete cracking due to tensile stresses at the bottom up to the shear debonding of the patches exhibit quite distinct acoustic signatures and can be identified. Waveform parameters such as duration and frequency content provide strong characterization capacity concerning the different processes. Valuable feedback is supplied by DIC (Digital Image Correlation) which verifies the moments of debonding by the significant strain release on the surface of the patch. Discussion is done on the in-situ application of this methodology and the limitations that may apply due to scattering and damping on the propagating waves.

Introduction

Characterization of acoustic emission (AE) waveforms relatively to the original failure mode enables evaluation of the structural condition. Usually in a concrete structure the fracture modes follow a sequence initiating with cracking due to tension and eventually leading to shear and related phenomena as the load increases. If the AE sources are characterized in a reliable way, this may act as warning against final failure. The AE technique utilizes suitable piezoelectric sensors to record the elastic waves emitted by the displacement of the crack tips and transform them in electric waveforms [1]. A typical waveform is depicted in Pic. 1. Some of the main characteristics are the highest amplitude of the waveform (amplitude, A in dB), the threshold crossings (else “counts”), the duration (delay between the first and last threshold crossing). Rise time (RT in μs) is the delay between the first threshold crossing and the peak point, while the basic frequency content is measured by average frequency (AF in kHz), which is the number of counts over the duration. Another parameter that has proven sensitive to the characterization of fracture mode is the RA value A in μs/V, standing for the ratio of RT over. The number and rate of incoming signals yields information on the active fracturing points and contributes to the monitoring of processes like fracture, creep, corrosion and self-healing [2-6]. Localization of the damage sources can also be conducted in one, two or three dimensions when numerous sensors are used [7]. Recently it was shown that AF decreases under shear mode of failure compared to tensile. Additionally, RA increases due to the higher percentage of shear waves emitted from a shear action [8]. These trends have been studied in laboratory with notable results regarding the original mode characterization of the AE sources [9-12]. In related standards for practical use [13] the classification is based on the AF-RA plot. There, the clusters of tensile and shear signals can be fully separated or by partial overlap [8-14].

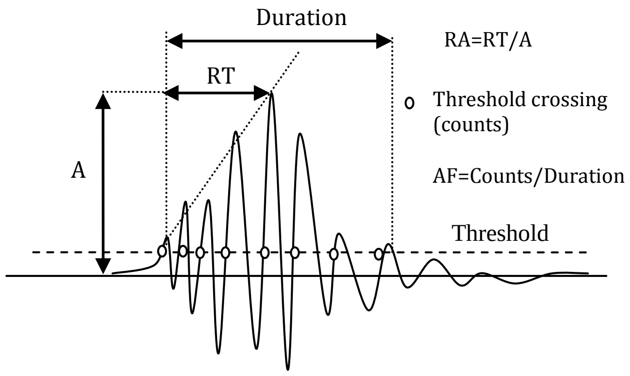

Pic 1. Typical AE signal and its main characteristics.

This paper presents the AE behavior under bending loading of concrete beams externally reinforced by patches such as carbon fiber reinforced plastics (CFRP) and textile reinforced cement (TRC).

The objective of the study is twofold. The first aim concerns the mechanical performance of the different reinforcement methods compared to a reference beam. Additionally, from the AE point of view, the external patches offer the possibility to monitor debonding activity and compare with the reference signals of concrete cracking. This carries strong importance since the patches are not transparent and therefore, assessment of the condition cannot be done by simple visual observation. AE was escorted by digital image correlation (DIC) in order to monitor the strain field in characteristic loading states. The combined DIC strain and AE activity information trends benchmarks the experimental results although no details are given in this manuscript. For the full combination study between AE and DIC the interested reader can consult [15, 16]. The effect of wave propagation is also discussed since in large scale, scattering and attenuation of AE waveforms will complicate any characterization attempt based on AE descriptors.

1. Experimental Details

1.1 Materials and Mechanical Test

Four-point bending tests were performed on three beam series with a total length of 2.5 m (middle span length of 2.3 m) height of 0.3 m and width of 0.2 m. The load was displacement controlled with an initial rate of 0.2 mm/min, while reaching the load of 60 kN the displacement rate was increased to 2.0 mm/min. The concrete used for the beams had compressive strength of 35.0 MPa and Young’s modulus of 34.0 GPa. Two steel bars (S500) of diameter 16 mm were used for internal reinforcement along with stirrups with diameter of 6 mm placed every 100 mm in the shear zones.

Concerning the external TRC reinforcement, it covered the whole bottom surface of the beam. It was made of an Inorganic Phospate Cement (IPC) matrix with 16 randomly oriented fibre textiles, resulting in a fibre volume fraction of 21%. At another beam, the CFRP strip placed (TRADECC 2007) was of thickness 1.2 mm and width of 30 mm. The tensile strength of the strip was 2210 MPa and the Young's modulus 143 GPa.

The external reinforcement was attached on the concrete surface with a two-component epoxy glue (PC 5800/BL) after removal of the laitance layer.

1.2 Acoustic Emission

In total eight AE sensors were attached on the central part of the beams. Five sensors were placed at the side, see Pic. 2, and three at the top surface. The other two sides were not available as they were covered and monitored by the DIC speckled pattern. Five of the sensors were of R15 type (Mistras) with resonance of 150 kHz and three were of the WD type with broadband response and center at 500 kHz. The sensors were placed at the center part of the beam spanning 150 mm to either side, with the lowest at 50 mm above the bottom, as seen in the photograph and the sketch of Pic. 2. The threshold was set at 35 dB, the pre-amplification at 40 dB and the signals were stored in a Mistras micro-II 8 channel system. This paper discusses mainly the results of the broadband sensors in order to have broader range of frequency values, while the resonant were very useful in capturing the load at the onset of cracking [15].

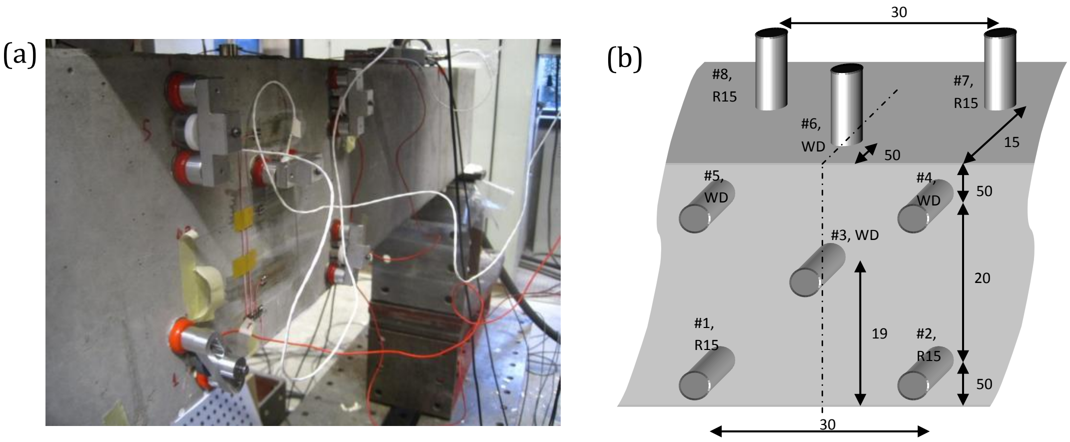

Pic. 2. (a) Photograph and (b) schematic representation of the experimental AE setup.

2. Results

From the total AE activity of the beams throughout loading, this paper focuses on specific moments when the load decreased, revealing a failure mechanism activation of high intensity. In all beams, as the mid-span deflection increased there were moments of temporary load drop, subsequently followed by the load regain. By comparing the strain on the reinforcing patches before and after, DIC aided in confirming that at those moments debonding of the external patch occurred [15]. Therefore, it was reasonable to compare the AE activity of those moments with the activity earlier or after the drops, when the dominant mechanism was concrete cracking.

Fig. 3a shows a part of the load history of the CFRP reinforced beam, along with the AF of the hits received by the broadband transducers. AF values were spread up to 300 kHz with the moving average line at approximately 90 kHz. At the moments of load drop (indicated by the arrows), a large group of lower frequency hits are registered (in the dash ellipse) causing a drop in the average line. Inversely, the RA value exhibited an increase at those moments as shown in Fig. 3b. Therefore, it is shown, that the activity during debonding is distinct from the concrete cracking and this can be utilized in cases of passive monitoring of composite structures, where visual observation and load readings are not available.

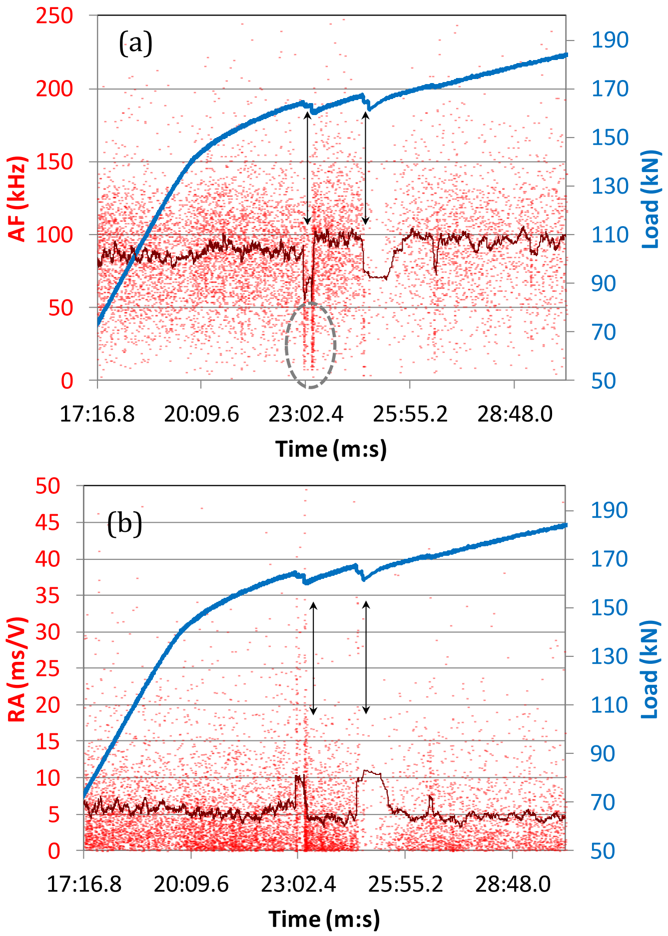

Pic. 3. Load history along with (a) AF, (b) RA value of the CFRP reinforced beam. The line is the moving average of 100 points.

To examine the AE activity in more detail, the population received during the load drops was compared with indicative parts of the population received during stable load increase. Pic. 4a shows the AF-Duration correlation plot for the CFRP beam. Despite the overlap, a shift towards lower frequencies and longer durations is noticed at the moments of load drop. It is characteristic that the average AF drops from 93 to 59 kHz while the average duration of AE signals increases from 467 to 1141 μs. Pics 4(b) and (c) show the corresponding plots for the TRC reinforced beams at the moments of temporary load drop. Again a strong shift is observed to lower frequencies and longer durations at the moments of load drop. Frequency decreases by 20 to 30 kHz while the duration increases by almost two to three times. It is mentioned that the TRC patch in the case of Pic. 4(c) was glued after a preloading to 40 kN in order to cause initial cracking before the application of the reinforcement. The shift of AE populations is noted in all cases, showing that it is due to the debonding action of either CFRP or TRC reinforcing. Therefore, in a monitoring case of similar nature, information on the condition of the structure may be possible by simply calling AE descriptors.

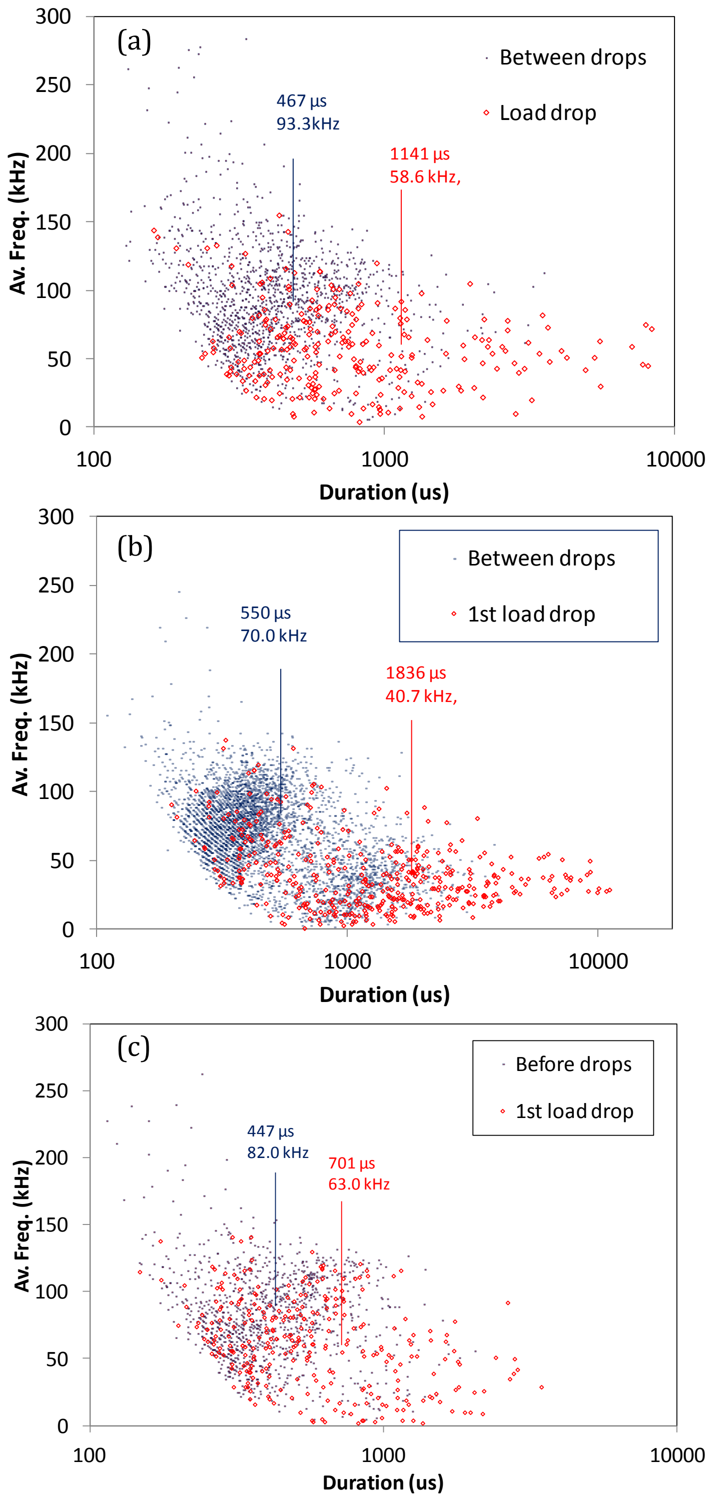

Pic. 4. AF-RA correlation plots for (a) CFRP beam, (b) TRC reinforced beam, (c) TRC reinforced pre-cracked beam.

3. Discussion on the Propagation Effect

The aim in this paper is not discriminating the mechanisms of fracture by means of pattern recognition algorithms. The essential objective is demonstrating that the raw waveforms as received by the sensors include valuable information regarding the failure mechanism. Under controlled conditions and further study a successful separation may be enabled. However, before this is done certain issues should be addressed. One is the effect of wave propagation which certainly attenuates the signal and masks the original waveform parameters. This is due to damping and scattering effects, strongly presented in a material as heterogeneous as concrete. It is well known that the frequency content of the waves decreases for long distances while their duration also changes (increases up to a distance) [17]. In order to see the influence of distance on the AE parameters, the location information from the AE "events" was utilized. The hits of each event were sorted according to their delay time between the different transducers that captured the event. Specifically, the hits were separated in groups according to their delay time. Pic. 5 shows the centers of the clusters for matrix cracking hits and CFRP debonding ones. Concerning the first (concrete cracking), the hits that were registered with small delay under 25 μs had an average AF of 97 kHz and RA of 2.9 ms/V. Considering a propagation velocity of 4000 m/s, this delay corresponds to events within a vicinity of 100 mm from the sensors. As the delay increases a smooth decrease of the frequency is noted accompanied by an increase of the average RA. For long distances of propagation (more than 500 mm or propagation delay longer than 125 μs) the average frequency is around 70 kHz and the RA value 9 ms/V. This shift masks the original characteristics of a concrete cracking signal and makes it resemble to a shear one, which anyway has lower frequency and higher RA. The corresponding shift of the debonding hits is also seen in the figure but it is not as strong as for the cracking ones.

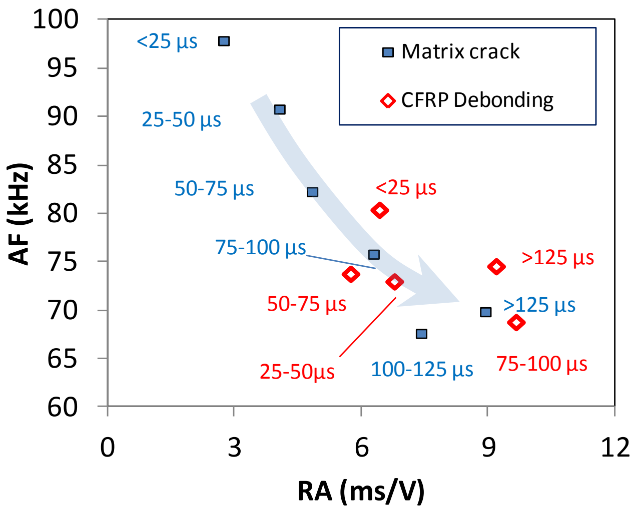

Pic. 5. Correlation plot of AF vs. RA for AE hits from CFRP debonding and concrete cracking.

4. Conclusions

The recent paper discusses results of bending on concrete beams externally reinforced by TRC or CFRP. It is shown that simple AE descriptors are sensitive to the change of the fracture mechanisms from cracking of concrete to debonding of the patches from concrete. Specifically cracking is characterized by higher frequency and relatively short AE waveforms, while at the moments of debonding the frequency drops by 30 to 50% and the duration increases by two to three times. Although these are strong indications that could assist a continuous structural health monitoring approach, the effect of propagation may pose serious problems in the evaluation in-situ. The reason is that the further the waves travel, their frequency is downshifted, while their energy components are delayed due to scattering resulting in longer waveforms. This makes the concrete cracking signals resemble shear and should be taken into account in order to lead to successful classification results.

References

1. C. U. Grosse, M. Ohtsu. (2008) Acoustic emission testing. Heidelberg: Springer.
2. I. Iturrioz, G. Lacidogna, A. Carpinteri. (2014) Acoustic emission detection in concrete specimens: Experimental analysis and lattice model simulations, International Journal of Damage Mechanics 23, 327-358
3. H. Cifuentes, B. L. Karihaloo. (2013) Determination of size-independent specific fracture energy of normal- and high-strength self-compacting concrete from wedge splitting tests, Construction and Building Materials 48, 548–553
4. E. Verstrynge, L. Schueremans, D. Van Gemert, M. Wevers. (2009) Monitoring and predicting masonry's creep failure with the acoustic emission technique. NDT&E International 42, 518–523
5. F. A. K. M. Uddin, M. Shigeishi, M. Ohtsu. (2006) Fracture Mechanics of Corrosion Cracking in Concrete by Acoustic Emission, Meccanica 41, 425–442
6. E. Tsangouri, D. G. Aggelis, K. Van Tittelboom, N. De Belie and D. Van Hemelrijck. (2013) Detecting the Activation of a Self-Healing Mechanism in Concrete by Acoustic Emission and Digital Image Correlation, The Scientific World Journal, Article ID 424560, http://dx.doi.org/10.1155/2013/424560
7. X. Luo, H. Haya, T. Inaba, T. Shiotani. (2006) Seismic diagnosis of railway substructures by using secondary acoustic emission, Soil Dynamics and Earthquake Engineering 26, 1101–1110
8. D. Polyzos, A. Papacharalampopoulos, T. Shiotani, D. G. Aggelis, (2011) Dependence of AE parameters on the propagation distance, Journal of Acoustic Emission, 29, 57-67
9. D. G. Aggelis. (2011) Classification of cracking mode in concrete by acoustic emission parameters, Mechanics Research Communications 38, 153-157
10. S. Shahidan, R. Pulin, N. Muhamad Bunnori,, K.M. Holford. (2013) Damage classification in reinforced concrete beam by acoustic emission signal analysis, Construction and Building Materials 45, 78–86
11. A. Farhidzadeh, E. Dehghan-Niri, S. Salamone, B. Luna, A. Whittaker. (2013) Monitoring crack propagation in reinforced concrete shear walls by acoustic emission, Journal of Structural Engineering, doi:10.1061/(ASCE)ST.1943-541X.0000781
12. T. Shiotani, Y. Oshima, M. Goto, S. Momoki. (2013) Temporal and spatial evaluation of grout failure process with PC cable breakage by means of acoustic emission, Construction and Building Materials 48, 1286-1292
13. M. Ohtsu. (2010) Recommendation of RILEM TC 212-ACD: acoustic emission and related NDE techniques for crack detection and damage evaluation in concrete: test method for classification of active cracks in concrete structures by acoustic emission, Materials Structure 43, issue 9, 1187–1189
14. K. Ohno, M. Ohtsu. (2010) Crack classification in concrete based on acoustic emission. Construction and Building Materials 24, 2339–46.
15. D. G. Aggelis, S. Verbruggen, E. Tsangouri, T. Tysmans, D. Van Hemelrijck. (2013) Characterization of mechanical performance of concrete beams with external reinforcement by acoustic emission and digital image correlation, Construction and Building Materials 47, 1037-1045
16. S. Verbruggen, D. G. Aggelis, T. Tysmans, J. Wastiels. (2014) Bending of beams externally reinforced with TRC and CFRP monitored by DIC and AE, Composite Structures 112, 113-121
17. T. Shiotani, D. G. Aggelis. (2009) Wave propagation in concrete containing artificial distributed damage. Materials and Structures 42, issue 3 , 377-384